



The role of excess MgO in the intensity increase of red emission of Mn⁴⁺-activated Mg₂TiO₄ phosphors

L. Borkovska¹ · L. Khomenkova¹ · I. Vorona¹ · V. Nosenko¹ · T. Stara¹ · O. Gudymenko¹ · V. Kladko¹ · C. Labbé² · J. Cardin² · A. Kryvko³ · T. Kryshtab⁴

Received: 18 October 2019 / Accepted: 18 February 2020 / Published online: 28 February 2020
© Springer Science+Business Media, LLC, part of Springer Nature 2020

Abstract

The influence of magnesium oxide (MgO) content on the intensity of red photoluminescence (PL) of Mn⁴⁺ ions in Mn-doped phosphors Mg₂TiO₄:Mn produced by solid-state reaction at 1200 °C has been investigated by PL, optical absorption, X-ray diffraction, and electron paramagnetic resonance methods. The phosphors synthesized with excess MgO show an increase of Mn⁴⁺ red emission compared with those of stoichiometric composition. The magnitude of this increase depends on both MgO and Mn content. The largest increase of PL intensity is found for the phosphors synthesized under 3:1 molar ratios of MgO to TiO₂. For these phosphors, the PL intensity increases from time 1.1 to time 3 when Mn concentration decreases from 1.0 to 0.0001 mol%. The phosphors produced under 6:1 molar ratios demonstrate a decrease of PL intensity at any Mn concentration. It is shown that excess MgO promotes stabilization of Mg₂TiO₄ phase against decomposition, hinders formation of Mn²⁺ centers, and enhances Mn⁴⁺ ions incorporation in the Mg₂TiO₄ crystal lattice. The latter together with reduced concentration quenching are supposed to be the main reasons of PL enhancement, which leads to the conclusion that excess MgO is necessary to produce an efficient red phosphor.

1 Introduction

Over the last decade, Mn⁴⁺-activated oxide and fluoride materials have attracted much interest as the cost-effective alternatives to rare-earth doped red phosphors for application in white light-emitting diodes (LEDs) [1]. The addition of red phosphor to Ce³⁺-activated yttrium garnet yellow phosphor excited by (Ga, In)N blue LED improves color rendering index and decreases correlated temperature of white LED [2]. All Mn⁴⁺-doped phosphors exhibit both broadband excitation in the ultraviolet-blue spectral region and narrow emission in the red that meet the spectral requirements for an ideal red-emitting phosphor for blue-chip excited white

LED. Today, Mn⁴⁺-activated fluorides demonstrate the highest quantum efficiency of about 98% [3] and found commercial application as red phosphors in white LEDs [4]. However, their use in high-power LEDs is largely impeded by their low thermal stability and insufficient humidity resistance. Moreover, toxic HF solution used in the synthesis process is harmful to the environment and human. On the contrary, Mn⁴⁺-activated oxides are distinguished by excellent stability and environmental safety.

Magnesium orthotitanate, Mg₂TiO₄, is considered as a proper host matrix for substitution of Ti⁴⁺ ions by Mn⁴⁺ ions since no charge compensation is needed. Mn⁴⁺-activated Mg₂TiO₄ shows intense emission peaked in the range of 565–560 nm that is both red and within the eye sensitivity curve [5–7]. The corresponding Commission Internationale de l'Éclairage (C.I.E.) chromaticity coordinate of this phosphor is (0.73, 0.26) that is better than commercial product Y₂O₂S:Eu³⁺ (0.64, 0.35) [8]. It has been shown that the Mg₂TiO₄:Mn⁴⁺ is a potential efficient red phosphor for application in InGaN blue-chip white LEDs to obtain a warmer white light emission with a higher color rendering index (CRI) and a lower correlated color temperature (CCT) [9, 10]. For example, it has been shown that the CRI of YAG:Ce³⁺-based white LED can be increased from

✉ L. Borkovska
l_borkovska@ukr.net

¹ V. Lashkaryov Institute of Semiconductor Physics of NASU, Pr. Nauky 41, Kiev 03028, Ukraine

² CIMAP, Normandie Univ, ENSICAEN, UNICAEN, CEA, CNRS, 6 Blvd. Maréchal Juin, 14050 Caen, France

³ Instituto Politécnico Nacional – ESIME Zacatenco, Av. IPN, Ed. Z4, U.P.A.L.M., 07738 Mexico City, Mexico

⁴ Instituto Politécnico Nacional – ESFM, Av. IPN, Ed.9 U.P.A.L.M., 07738 Mexico City, Mexico

68.1 to 79.8 with the CCT decreasing from 6565 to 4344 K when $\text{Mg}_2\text{TiO}_4:0.1\%\text{Mn}^{4+}, 0.4\%\text{Zn}^{2+}$ red phosphor is added [10] as well the CCT can be decreased to 4270 K when $\text{Mg}_2\text{TiO}_4:\text{Mn}^{4+}, \text{Bi}^{3+}, \text{Li}^+$ red phosphor is introduced [9]. The $\text{Mg}_2\text{TiO}_4:\text{Mn}^{4+}$ phosphors can be fabricated easily by classical solid-state reaction via sintering of magnesium oxide (MgO) and titanium dioxide (TiO_2) powders in the air [7–12]. The reduced pollution, low cost, simplicity in process and handling, and ability to produce materials in large quantities make this method practical for the low-cost mass production. However, the quantum efficiency of $\text{Mg}_2\text{TiO}_4:\text{Mn}^{4+}$ red phosphor is still too low for commercial application in white LEDs [6] and needs therefore to be improved.

The method of solid-state reaction is known to be highly sensitive to process conditions. In particular, for sintering of $\text{Mg}_2\text{TiO}_4:\text{Mn}^{4+}$ phosphors, the annealing temperatures in the range of 1250–1400 °C are usually used [8–11]. However, the sintering of $\text{Mg}_2\text{TiO}_4:\text{Mn}^{4+}$ at temperatures higher than 1200 °C results in weaker intensity of red emission [7]. Different technological approaches were proposed for the increasing of intensity of Mn^{4+} photoluminescence (PL) in oxide matrices, including additional annealing in oxygen flow [8], adding of fluxes [13] and co-doping [14]. Specifically, it has been shown that, the intensity of Mn^{4+} emission in $\text{Mg}_2\text{TiO}_4:\text{Mn}^{4+}$ can be increased by co-doping with metal ions such as $\text{Li}^+, \text{Zn}^{2+}, \text{Nb}^{5+}, \text{Bi}^{3+}$. [9, 10, 12, 15]. The role of co-dopant has been assigned to the flux effect [10, 12] and to the formation of Ti vacancies [15]. It has been shown that the introduction of a small amount of MgO into Mn^{4+} -activated $\text{CaAl}_{12}\text{O}_{19}$ [16], $\text{Sr}_4\text{Al}_{14}\text{O}_{25}$ [17], and LiGaTiO_4 [18] red phosphors results in an increase of the PL efficiency. Although no satisfactory explanation of this effect has been proposed yet, some authors consider that Mg^{2+} ion substitutes one of the Mn^{4+} ions in close $\text{Mn}^{4+}\text{--Mn}^{4+}$ pair connected with O^{2-} impurity and reduces the effect of luminescence quenching [16]. However, possible influence of MgO on the PL intensity of Mn^{4+} -activated Mg_2TiO_4 phosphor has not been investigated.

Hereafter, the results of optical and structural studies of Mn-doped Mg_2TiO_4 red phosphors produced through a classical solid-state synthesis under excess MgO are presented and the conditions for improvement of Mn^{4+} red PL are proposed.

2 Experimental details

The phosphors were obtained by a classical solid-state reaction method. The raw MgO and TiO_2 powders were weighted in different molar ratios: mol MgO: mol $\text{TiO}_2 = 2:1, 3:1$ and $6:1$. The 2:1 molar ratios correspond to stoichiometric composition of Mg_2TiO_4 , and the other two result in

the multicomponent phosphors with Mg_2TiO_4 and excess MgO phases, respectively. A saturated aqueous solution of manganese sulfate (MnSO_4) was diluted with distilled water in different ratios and added to powder mixture to provide a nominal Mn content, N_{Mn} , of 0.0001, 0.1, and 1.0 mol% assuming that Mn substitute Ti site atoms only. After a thoroughly mixing, the pellets of the average size of about $10 \times 5 \times 5 \text{ mm}^3$ were formed from the powder mixture. The pellets were dried in air at 200 °C for 3 h and then sintered in air at 1200 °C for 3 h. The ceramic samples were cooled naturally with furnace cooling down. Two sets of phosphors with Mn content of 0.0001 and 0.1 mol% and molar ratios mol MgO: mol $\text{TiO}_2 = x:1$, where x varied in the range (2.4–4), were also produced in the same manner.

The PL spectra were recorded using an SDL-23 spectrometer (LOMO, St. Petersburg) equipped with a photomultiplier tube and excited by a 409 nm continuous diode laser (50 mW). In the case of PL excitation spectra study, the optical excitation source was the Lot-Oriel 1 kW Xenon white lamp with an OMNI300 monochromator selecting the wavelength. For PL relaxation investigation, the 337.1 nm line of pulse N_2 -laser was used as an excitation source. The PL spectra were studied both at room and at liquid nitrogen temperature, and the PL relaxation was recorded at room temperature only. The diffuse reflectance spectra were recorded using a Cary 4000 UV–Vis spectrophotometer (Varian). The optical absorption spectra were recalculated from the diffuse reflectance spectra using the Kubelka–Munk theory. The X-ray diffraction (XRD) study was realized in the $\theta\text{--}2\theta$ geometry using High-Resolution Philips X'Pert PRO MRD diffractometer with $\text{CuK}\alpha_1$ radiation. The topology of sintered ceramic samples was investigated by scanning electron microscopy (SEM) using High-resolution scanning electron microscope Tescan Mira 3 LMU. The elemental analysis of ceramic surface was realized by Energy dispersive X-ray spectrometry (EDX) using Oxford Instruments energy dispersive spectrometer Oxford Instruments X-Max 80. Electron paramagnetic resonance (EPR) study was carried out using X-band EPR spectrometer Varian E12 (~9.5 GHz) equipped by paired cavity that allows recording EPR signals from a standard (a Mn-doped MgO sample) and a phosphor separately by modulation switching. The EPR spectra were normalized with respect to the intensity of the signal of a standard, as well as on the mass of each sample studied.

3 Experimental results

3.1 Scanning electron microscopy and elemental analysis investigations

Figure 1 shows SEM images of cleaved ceramic surfaces of 1% Mn-doped phosphors synthesized under different

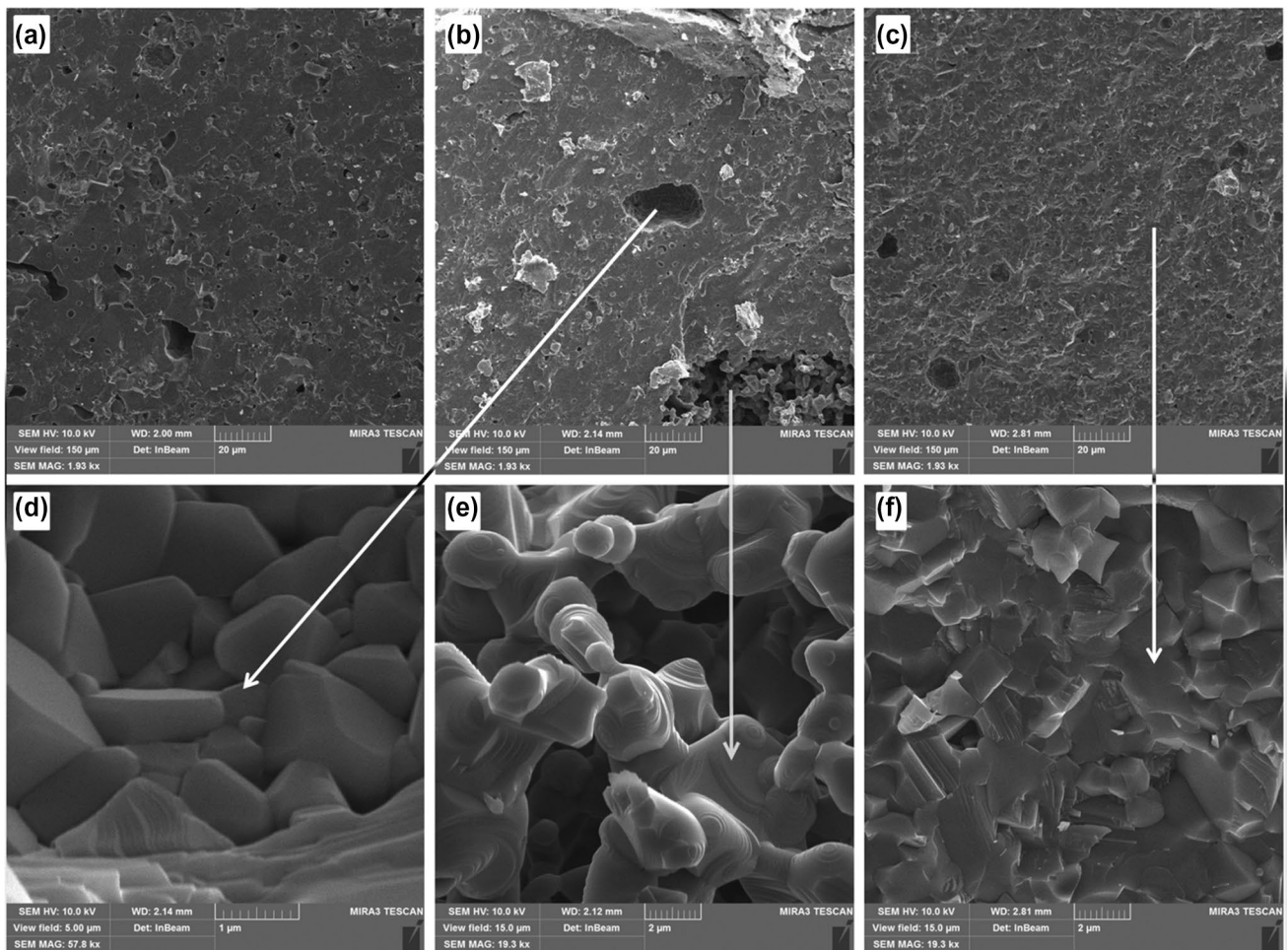


Fig. 1 SEM micrographs of the cleaved ceramic surfaces of the $\text{Mg}_2\text{TiO}_4\text{:Mn}^{4+}$ phosphors with $N_{\text{Mn}} = 1\%$ and different MgO-to- TiO_2 molar ratios: 2:1 (a), 3:1 (b) and 6:1 (c) as well as the enlarged sur-

face microstructures in pores of different types of the phosphor produced under 3:1 ratio (c, d) and cleaved surface of phosphor synthesized under 6:1 ratio (e)

MgO-to- TiO_2 molar ratios. All the ceramics demonstrate relatively dense and fine-grained microstructures and the presence of rare not spherical pores (Fig. 1a–c). The pores of two types were revealed. The pores of the first type of sizes ranging from 2 to 20 μm were observed in all samples and contained faceted crystal grains of μm sizes related apparently to Mg_2TiO_4 (Fig. 1d). The pores of second type reached 80 μm in diameter and were found in the phosphor produced under 3:1 molar ratio only. They also contained crystal grains of μm sizes of different shape (Fig. 1e). The EDX analysis of the regions inside these pores found the decreased concentration of Ti ([Mg] = 62 at.%, [Ti] = 1 at.%, [O] = 38 at.%) which allows ascribing them to MgO inclusions. In addition, the EDX spectra recorded in different points of the sample outside the pores showed varied ratio of Mg to Ti elements (point 1: [Mg] = 39 at.%, [Ti] = 19 at.%, [O] = 51 at.%; point 2: [Mg] = 34 at.%, [Ti] = 15 at.%, [O] = 51 at.%). This indicates non-uniform distribution of excess MgO in the phosphor. Analysis of the EDX spectra

measured in tightly sintered regions of the samples demonstrated the decrease of relative intensity of Ti peak as the excess MgO content increases (from [Mg] = 36 at.%, [Ti] = 18 at.%, [O] = 46 at.% in the sample produced under 2:1 molar ratio to [Mg] = 43 at.%, [Ti] = 11 at.%, [O] = 46 at.% in the sample synthesized under 6:1 ratio). It can be supposed that excess MgO not only forms relatively large inclusions inside the ceramic pellets but also produces smaller MgO crystal grains sintered with the Mg_2TiO_4 ones. It should be noted that, no Mn-rich inclusions were found in the elemental analysis of the cleaved ceramic surfaces. This implies relatively homogeneous distribution of dopant inside the pellets.

3.2 XRD study

The XRD patterns of the phosphors of stoichiometric (2:1) composition (Fig. 2a, b) reveal intense peaks caused by reflections of cubic Mg_2TiO_4 phase (JCCD PDF

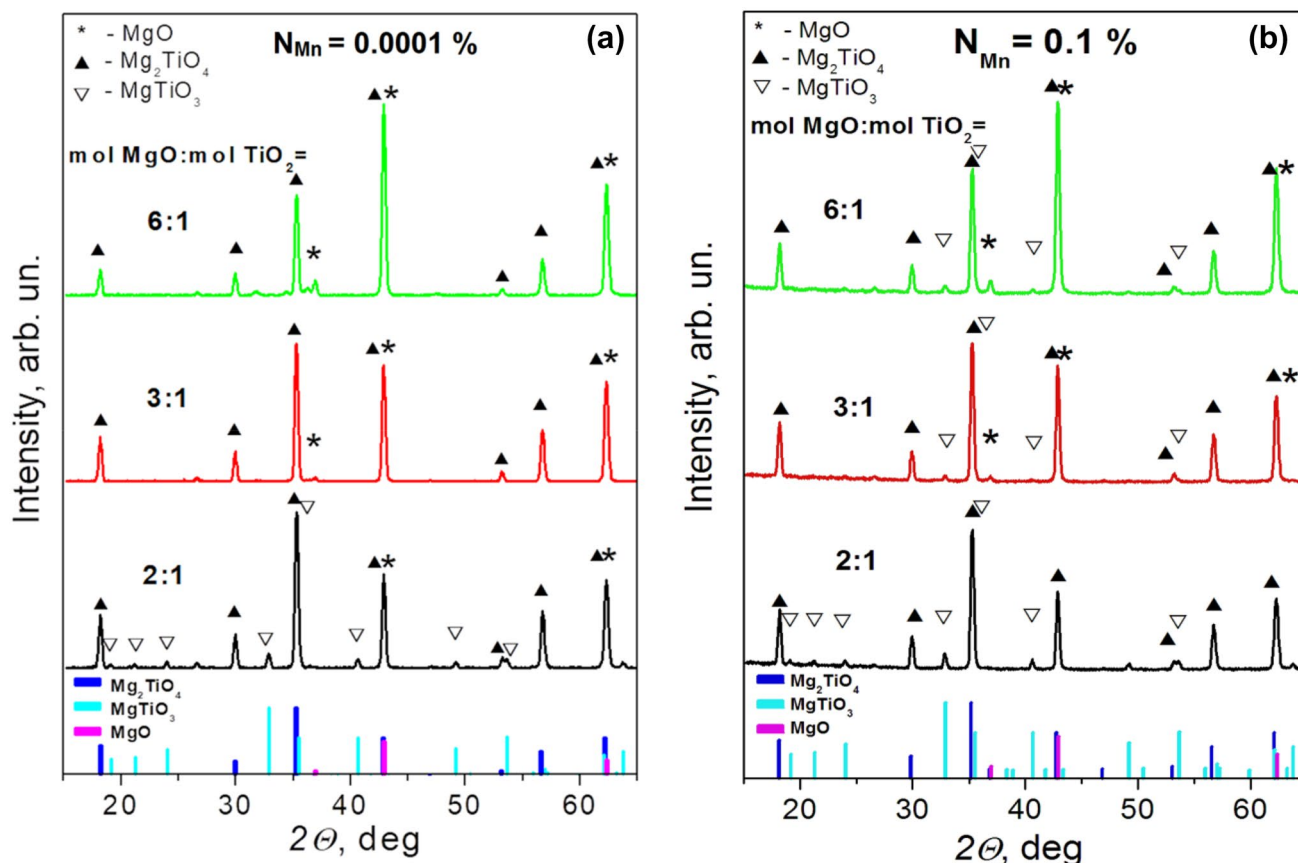


Fig. 2 XRD patterns of the phosphors with $N_{\text{Mn}}=0.0001\%$ (a) and 0.1% (b) produced under different MgO-to-TiO₂ molar ratios, and the simulated XRD patterns for MgO (PDF 010-77-2364), Mg₂TiO₄ (PDF 01-079-0830), and MgTiO₃ (PDF 01-075-3957)

000-25-1157) and the peaks of lower intensity of rhombohedral MgTiO₃ phase (JCD D PDF 010-75-3957). The concentrations of these phases estimated by the Reference intensity ratio method were about 90 and 10%, respectively.

It is well established that MgTiO₃ accompanies formation of Mg₂TiO₄ at temperatures lower than 1400 °C [19] following the decomposition reaction $\text{Mg}_2\text{TiO}_4 = \text{MgTiO}_3 + \text{MgO}$ [20]. However, it has been proposed also [19] that Mg₂TiO₄ decomposes on Mg-rich spinel and MgTiO₃ as $\text{Mg}_2\text{TiO}_4 = \text{Mg}_{2+2i}\text{Ti}_{1-\delta}\text{O}_4 + \text{MgTiO}_3$. This was concluded from the fact that the peaks of MgO were not observed in the XRD patterns. We also do not find the peaks of crystalline MgO phase in the XRD patterns of the phosphors of stoichiometric composition. Although it is worth noting that, the most intense peaks of cubic MgO strongly overlap with those of cubic Mg₂TiO₄, which complicates making precise conclusion about the presence of MgO. At the same time, a clear peak at 36.96 degrees of low intensity for (111) reflection of the crystalline MgO appears only in the XRD patterns of the phosphors produced with excess of MgO. It is hardly believed that some preferred grain orientation for $\langle 111 \rangle$ planes of MgO phase is present only in the phosphors

produced with excess of MgO and is absent in the phosphors of stoichiometric composition. So, it can be concluded that MgO phase is not formed in the phosphors of stoichiometric composition that correlates with the SEM investigations.

The XRD studies show that excess MgO hinders the decomposition of Mg₂TiO₄ (Fig. 2a, b). In the samples prepared with excess MgO, the MgTiO₃ phase is not formed at all in the case of low Mn concentrations ($N_{\text{Mn}}=0.0001\%$) or formed in a smaller amount in the samples with higher Mn concentrations ($N_{\text{Mn}}=0.1\%$). In the last case, the appearance of MgTiO₃ phase can be due to a complex effect of Mn dopant on Mg₂TiO₄ decomposition. The XRD study allows estimation of size of perfect crystallites (coherent domains). The average crystallite sizes (D) was evaluated from the full width at a half maximum (FWHM) of the most intensive (311) diffraction peak of Mg₂TiO₄ using the Scherrer equation [21]: $D(2\theta) = K\lambda/(\beta(2\theta)\cos\theta)$, where $\lambda = 1.540562 \text{ \AA}$ and is the X-ray wavelength, $\beta(2\theta)$ is the FWHM, $K=0.9$ and is the shape factor. As the diffraction patterns were recorded using XRD Panalitical Xpert PRO MRD diffractometer with the instrumental line broadening $\beta_{\text{inst}}=0.08^\circ$ (0.0014 Rad), its contribution to $\beta(2\theta)$ was negligible. The average

coherent domain sizes remain in the 29–31 nm range. As only one peak was used for size evaluation, the line broadening caused by residual strains was not taking into account. This results in somewhat underestimation of crystallite sizes.

The values of coherent domain sizes are more than ten times smaller than grain sizes obtained from SEM images (about microns). This means that observed grains contain extended defects (dislocations, subgrain boundaries) with a high density. In fact, some roughness of the surface of the grains is observed (Fig. 1), which confirms that the grains are the conglomerates of crystallites (coherent domains).

3.3 Photoluminescence and optical absorption investigations

The room temperature PL spectra of all phosphors (Fig. 3a–c) show the PL bands in the red spectral range with the most intense one peaked at 660 nm and ascribed to spin forbidden ${}^2E_g \rightarrow {}^4A_{2g}$ transitions of the Mn^{4+} ions in octahedral symmetry substituted Ti^{4+} ions in crystal lattice of Mg_2TiO_4 . The corresponding PL caused by Mn^{4+} ions in $MgTiO_3$ is found at about 701 nm [12] as a hump of low intensity apparently because of low concentration of this phase.

The PL study reveals that excess MgO affects the intensity of Mn^{4+} red PL. The PL intensity of the phosphors synthesized under 3:1 ratio increases by 10 to 300% as compared with those of stoichiometric composition. The

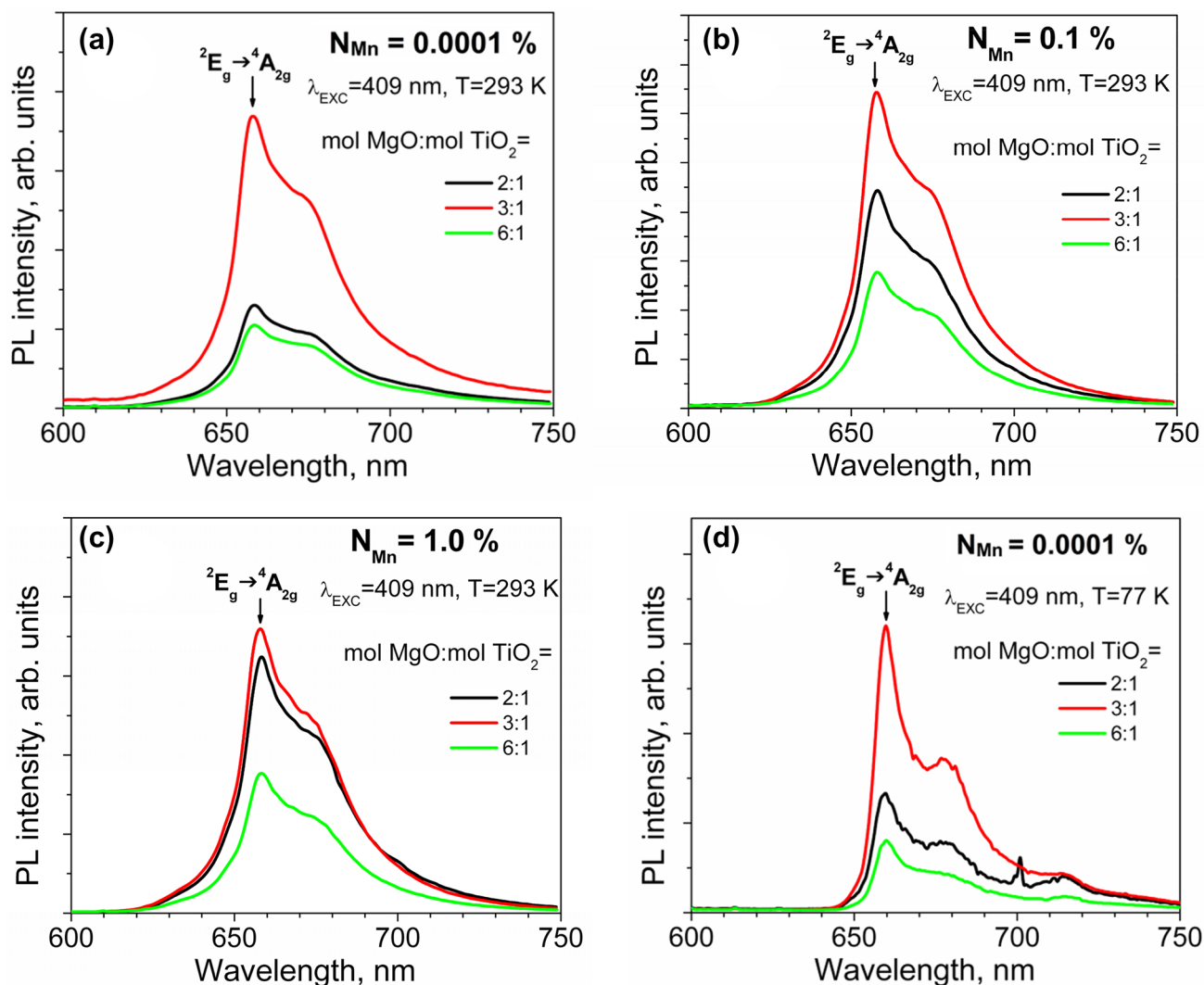


Fig. 3 Room temperature (a–c) and low-temperature (d) PL spectra of the phosphors with $N_{Mn}=0.0001\%$ (a, d), 0.1% (b), and 1.0% (c) produced under different MgO-to-TiO₂ molar ratios

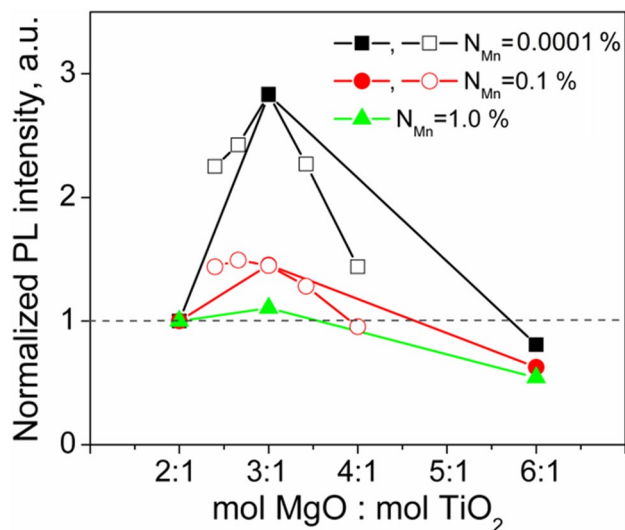


Fig. 4 Normalized intensity of Mn^{4+} red PL versus MgO content in the phosphors with different doping level. The solid lines are drawn for better eye guide

largest magnitude of the effect is for the lowest Mn-doping level ($N_{\text{Mn}}=0.0001\%$) and decreases as the Mn content increases (Fig. 4). At the same time, the phosphors produced under 6:1 molar ratio demonstrate up to two times lower PL even compared to the phosphors of stoichiometric composition. The PL spectra of the set of phosphors with smaller step of MgO excess show that the optimal ratio to produce the phosphor with the largest PL intensity is in the range of (2.6 ÷ 3):1, the higher is Mn content, the lower should be the excess MgO content. For $N_{\text{Mn}}=0.1\%$, that is close to critical concentration of Mn^{4+} in Mg_2TiO_4 [8, 11], the PL intensity can increase in 1.5 times. The low-temperature PL spectra (Fig. 3d) reveal similar changes of the PL intensity versus excess MgO content as the room temperature PL spectra, i.e., the phosphors produced under 3:1 ratio show an increased PL and those made under 6:1 molar ratio demonstrate a decreased red PL.

The PL relaxation curves of the phosphor of stoichiometric composition and the one produced with excess MgO (3:1 ratio) are shown in Fig. 5. The curves do not show single-exponential behavior and have been approximated by double-exponential function as $W(t) = A_1 \exp(-t/\tau_1) + A_2 \exp(-t/\tau_2)$, where $W(t)$ refers to the PL intensity at time t , A_1 and A_2 are constants, and τ_1 and τ_2 are the decay times of the two components. The approximation gives decay times of 498 and 508 μs for slower component, and 87 and 100 μs for faster component in the phosphors of stoichiometric composition and in the phosphors produced under 3:1 molar ratio, respectively. The decay times of slower component agree well with those reported by other authors for room temperature Mn^{4+} red PL in Mg_2TiO_4 [11].

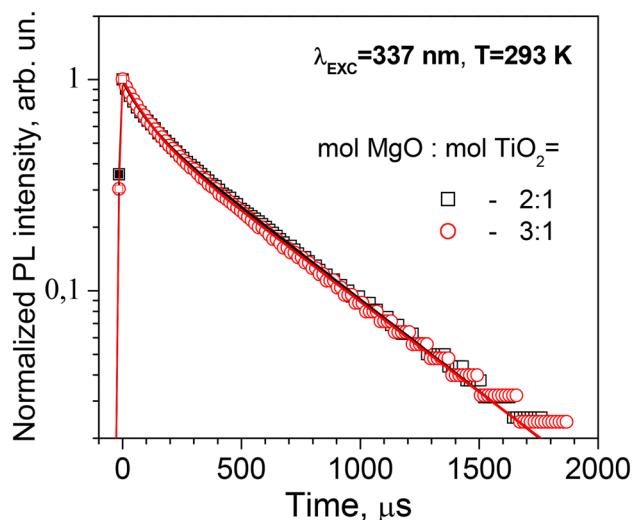
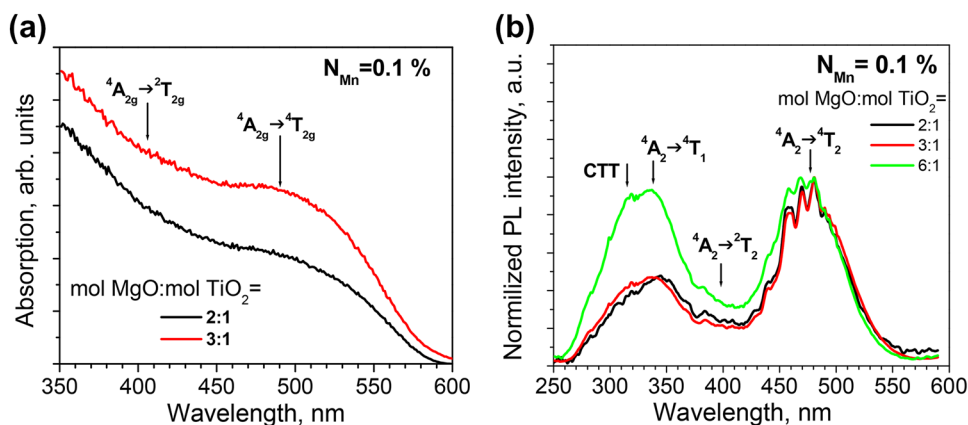


Fig. 5 Decay curves of normalized PL intensity monitored at 660 nm in Mn-doped phosphors ($N_{\text{Mn}}=0.0001\%$) produced under different molar ratios of MgO to TiO_2

In general, the PL relaxation time, τ , can be expressed as $1/\tau = 1/\tau_{\text{R}} + 1/\tau_{\text{NR}}$, where τ_{R} is the radiative decay time and τ_{NR} is the non-radiative decay time. The second term reflects contribution of thermal quenching as well as the energy transfer from Mn^{4+} ion to the centers of non-radiative recombination. The latter are considered to be Fe^{3+} ions [22] or Mn ions in other valence states than +4 [23]. The multi-exponential behavior of PL relaxation is often observed in Mn-doped compounds [23, 24] and can be caused by non-equivalent surroundings of Mn^{4+} centers. In particular, incorporation of Mn^{4+} ions in close vicinity of another point defect can affect radiative recombination time [25, 26] or promote quenching of Mn^{4+} emission via metal-to-metal charge states or direct energy transfer [23]. In the proximity of Mn^{4+} ions, where energy migration is possible, the contribution of non-radiative recombination will increase and PL relaxation time τ become shorter. Small increase of relaxation times in the phosphors synthesized under 3:1 molar ratio most likely indicates a decrease of contribution of non-radiative recombination in the PL relaxation. This can be caused by the decrease of concentration of the centers on non-radiative recombination as well as by reduced energy migration owing to more uniform distribution of Mn^{4+} ions in Mg_2TiO_4 grains.

The phosphors produced under 3:1 molar ratio demonstrated not only higher PL intensity but also more saturated color than those made under 2:1 and 6:1 ratios. The changes in the phosphor color were noticeable in the eye. Optical absorption spectra show that this is due to more intense absorption caused by Mn^{4+} ions in Mg_2TiO_4 phase (Fig. 6a). In fact, the absorption edge of the phosphors in the visible spectra range is determined by the broad absorption band

Fig. 6 Optical absorption spectra (a) and PL excitation spectra (b) of Mn-doped phosphors ($N_{\text{Mn}}=0.1\%$) produced under different molar ratios of MgO to TiO_2



peaked at about 490 nm, which originates from ${}^4\text{A}_{2g} \rightarrow {}^4\text{T}_{2g}$ spin-allowed transitions of Mn^{4+} in Mg_2TiO_4 . The identification of the absorption bands is consistent with the excitation spectra of Mn^{4+} emission (Fig. 6b). In the phosphors produced under 3:1 molar ratio, the intensity of this absorption increases noticeably. This allows concluding that excess MgO stimulates formation of Mn^{4+} centers in Mg_2TiO_4 .

3.4 EPR study

The X-band EPR spectra of the phosphors of stoichiometric composition are presented in Fig. 7a. Each spectrum shows several EPR sextets with the g factor of about 2.0 caused by the interaction of electron–nuclear spins of Mn^{2+} ions in MgTiO_3 and Mg_2TiO_4 phases. The EPR signal due to Mn^{2+} ions in MgO phase was not detected that is consistent with the XRD results. The experimental spectra were simulated using the powder program included in the Visual-EPR program package [27]. The spin-Hamiltonian parameters of Mn signals, such as the fine constant D and hyperfine constant A, were found to be $165 \times 10^{-4} \text{ cm}^{-1}$ and $79 \times 10^{-4} \text{ cm}^{-1}$

for MgTiO_3 , and $60 \times 10^{-4} \text{ cm}^{-1}$ and $74 \times 10^{-4} \text{ cm}^{-1}$ for Mg_2TiO_4 , respectively. The simulations of Mn^{2+} signals in MgO, MgTiO_3 , and Mg_2TiO_4 phases are presented in Fig. 7b.

The EPR signal that can be ascribed to Mn^{4+} ions in MgTiO_3 and Mg_2TiO_4 phases was not detected. Most likely, this is because of unfavorable relaxation conditions of Mn^{4+} ions in magnesium titanates (too short or too long spin relaxation times). The EPR spectra (Fig. 7a) show that the increasing of Mn-doping level produces the increase of Mn^{2+} ion content in both titanate phases. The concentrations of Mn^{2+} ions estimated from the EPR spectra are found to be more than ten times smaller than corresponding Mn content.

An excess MgO leads also to noticeable changes in the EPR spectra (Fig. 8). Firstly, an intense signal caused by Mn^{2+} ions in MgO phase arises and increases in intensity as the MgO content increases. Secondly, the EPR signal of Mn^{2+} ions in MgTiO_3 disappears. Since at least some of these phosphors contain MgTiO_3 phase (Fig. 2b), it can be concluded that excess MgO completely suppresses the formation of Mn^{2+} centers in MgTiO_3 . Thirdly, the EPR signal

Fig. 7 Experimental EPR spectra of Mn-doped phosphors of stoichiometric composition with different doping level (a) and simulated EPR signals of Mn^{2+} ions in MgO, MgTiO_3 , and Mg_2TiO_4 phases (b)

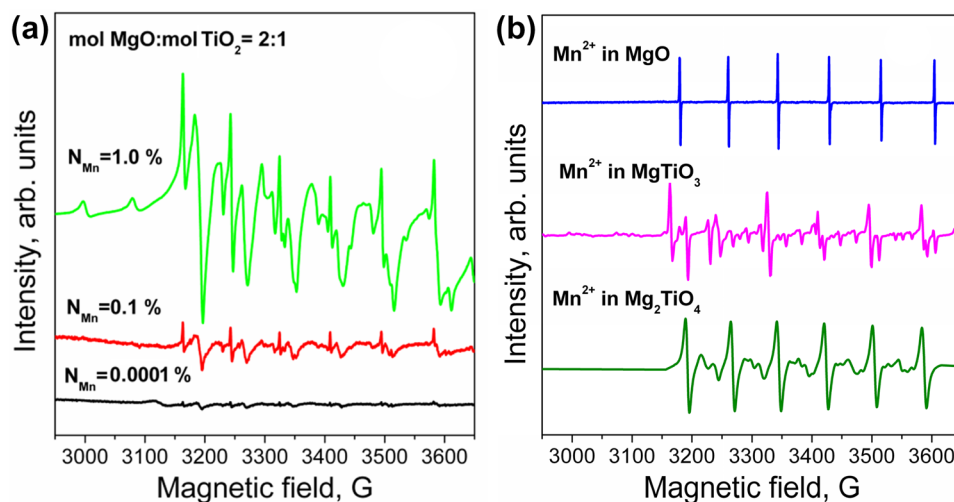
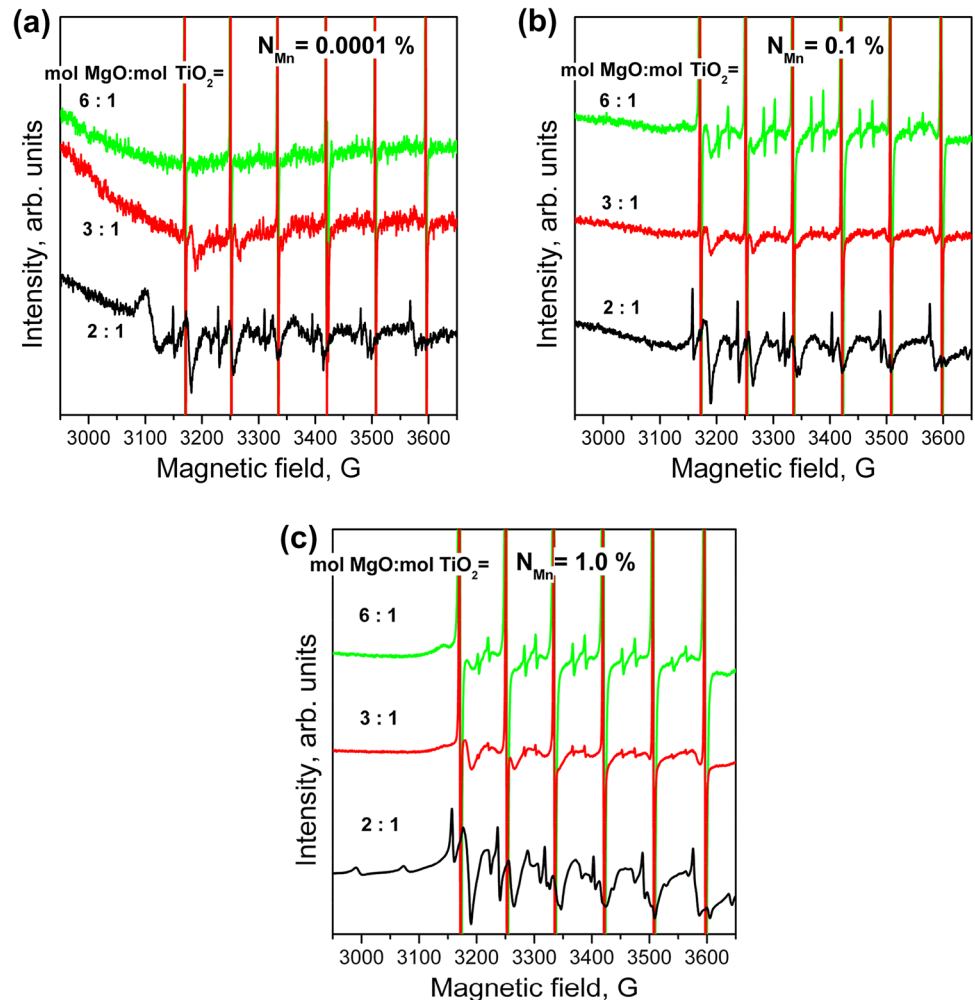


Fig. 8 Experimental EPR spectra of the phosphors with Mn nominal content of 0.0001% (a), 0.1% (b), and 1.0% (c) produced under different molar ratios of MgO to TiO₂



caused by Mn²⁺ ions in Mg₂TiO₄ decreases in intensity. This suggests that excess MgO hinders formation of Mn²⁺ centers in both titanate phases.

4 Discussion

The obtained results show that an excess MgO has complex effect on phase stabilization and Mn incorporation in magnesium titanate crystal phases. Specifically, the XRD reveals that excess MgO hinders decomposition of Mg₂TiO₄. One of the possible explanations can be that excess MgO affects the surface energy of Mg₂TiO₄ grains. For nanosized grains, the surface energy contributes distinctly into free energy term. The effect is noticeable when the grain size is lower than 30 nm [28]. In our phosphors, the grain size of Mg₂TiO₄ phase evaluated from the FWHM of corresponding XRD peak is about 30 nm. Therefore, the changes in surface energy of titanate grains can influence Mg₂TiO₄ decomposition. In fact, both MgO and Mg₂TiO₄ have cubic structure. Moreover, the unit cell parameter of MgO is half of that of

Mg₂TiO₄. Thus, they may form coherent structures, which save surface energy of Mg₂TiO₄ grain. On the contrary, the rhombohedral MgTiO₃ and cubic MgO phases require incoherent boundaries. Therefore, an excess MgO can be efficient in the stabilization of Mg₂TiO₄ phase. Another possible role of excess MgO in stabilization of Mg₂TiO₄ phase can be related to its effect on intrinsic defect formation, in particular on concentration of oxygen vacancies. In fact, stabilization of cubic/tetragonal crystal phase of other oxide-based materials (for instance, HfO₂ and ZrO₂) via doping with subvalent impurities is known to be associated with introduction of intrinsic defects, such as oxygen vacancies, required for charge compensation [29, 30].

An excess MgO also affects Mn incorporation in magnesium titanate phases and promotes PL intensity increase. In general, the increase of PL intensity can be caused by (i) an increase in concentration of Mn⁴⁺ centers and (ii) a decrease of non-radiative recombination that affects Mn⁴⁺ emission. The first process apparently contributes to the PL enhancement in the phosphors studied. The optical absorption spectra show an increased absorption of Mn⁴⁺ ions in

the phosphors synthesized under excess MgO. This implies that excess MgO stimulates formation of “additional” Mn^{4+} centers in the Mg_2TiO_4 phase. The source of these “additional” ions can be some residuary Mn compounds or manganese ions incorporated in Mg_2TiO_4 in other charge states than +4. In fact, the EPR spectra show that in the phosphors synthesized under 3:1 molar ratio, the concentration of Mn^{2+} ions in Mg_2TiO_4 phase decreases. The reason can be the diffusion of Mg^{2+} ions from MgO into Mg_2TiO_4 and substitution of Mn^{2+} ions on lattice sites. Similarly, the improvement of PL intensity of Mn-doped $\text{CaAl}_{12}\text{O}_{19}$ due to MgF_2 addition has been explained by the increment of the fraction of Mn ions in the +4 charge state due to the incorporation of Mg^{2+} instead of Mn^{2+} [31].

However, if the increase of Mn^{4+} ions content is the only reason of PL increase, the intensity of Mn^{4+} emission in the phosphors with nominal Mn content of 1.0 and 0.1% should decrease upon MgO adding. This is because of the concentration quenching of Mn^{4+} PL occurred at $N_{\text{Mn}} > 0.1\%$. At the same time, an increase of PL intensity is found. This means that a decrease of contribution of non-radiative recombination takes place. At room temperature the latter occurs via thermal quenching of PL intensity and energy exchange between Mn^{4+} ions via electric dipole–dipole or exchange interaction following by energy transfer to the center of non-radiative recombination. According to the Struck-Fonger model [32], thermal quenching occurs due to the increasing probability of tunneling of charge carrier from a vibrational level of the excited state to a high vibrational level of the ground state. It is unlikely that the incorporation of Mg^{2+} into crystal lattice of magnesium titanates affects this process. In fact, the low-temperature PL spectra of the phosphors with the same doping level show similar dependence of PL intensity on the excess quantity of MgO as the room temperature spectra. This means that the thermal quenching of PL intensity does not change with MgO addition. In turn, Mg^{2+} can affect the energy exchange between Mn^{4+} ions and concentration of non-radiative defects. In general, Mg^{2+} can substitute both Mn^{2+} and Mn^{4+} ions in the crystal lattice of magnesium titanate. If Mg^{2+} substitutes one Mn^{4+} in close Mn^{2+} – Mn^{4+} pair, it will prevent the energy exchange between the ions, thus enhancing the Mn^{4+} PL efficiency [16]. If Mg^{2+} substitutes Mn^{2+} ion in close Mn^{2+} – Mn^{4+} pair, it will impede energy transfer from Mn^{4+} to Mn^{2+} followed by non-radiative recombination. In fact, it has been proposed that the quenching of Mn^{4+} luminescence can occur via metal-to-metal charge-transfer or direct energy transfer from Mn^{4+} to Mn^{2+} and Mn^{3+} ions [23, 33]. In this case, the decrease of concentration of Mn ions in charge states other than +4 can decrease the number of the centers of non-radiative recombination and increase the Mn^{4+} PL efficiency. It can be concluded that excess MgO not only increases the number of Mn^{4+} ions but also decreases the

effect of non-radiative recombination on Mn^{4+} emission. The latter presumably occurs via more uniform distribution of Mn^{4+} ions and/or decreasing the number of Mn ions in charge states other than +4 acting as the centers of non-radiative recombination.

The obtained results indicate that the intensity of Mn^{4+} emission in Mg_2TiO_4 can be increased up to 3 times upon MgO adding. This effect seems to be very promising for practical application of the phosphors for lighting. An excess MgO stimulates incorporation of manganese in Mg_2TiO_4 in +4 charge state and decreases concentration of Mn^{2+} centers upon sintering at 1200 °C. This allows producing red phosphors at temperatures that do not exceed 1200 °C and eliminates the necessity of additional annealing in oxygen. We suppose that the using of excess MgO allows decreasing the cost and time of phosphor production.

5 Conclusion

The effect of excess MgO with respect to the stoichiometric Mg_2TiO_4 composition on the intensity of red emission in Mn^{4+} -activated Mg_2TiO_4 phosphors has been investigated. The phosphors were synthesized via solid-state reaction at 1200 °C in the air under molar ratios of MgO to TiO_2 varied in the range from 2:1 to 6:1. The XRD study revealed that excess MgO hindered the decomposition of Mg_2TiO_4 on MgTiO_3 and MgO. It is supposed that excess MgO saves the surface energy of Mg_2TiO_4 grain and stabilizes Mg_2TiO_4 phase.

The optical study showed that additional MgO promoted the incorporation of Mn in +4 charge state in both Mg_2TiO_4 and MgTiO_3 phases. This is proved by the increase of optical absorption and PL intensity caused by Mn^{4+} ions in Mg_2TiO_4 , as well as by a decrease of the EPR signal due to Mn^{2+} ions in Mg_2TiO_4 crystal phase. The EPR signal of Mn^{2+} ions in MgTiO_3 disappeared. This implies that excess MgO completely suppresses the incorporation of Mn in +2 charge state in MgTiO_3 . The effect is ascribed to the diffusion of Mg^{2+} ions from MgO into titanate phases and the substitution of Mn^{2+} ions on the lattice sites.

The PL intensity was found to depend non-monotonously on the quantity of additional MgO. The largest increase of PL intensity was found for molar ratios (2.6–3.0):1 and its magnitude varied in 1.1–3 times depending on Mn content, namely the larger was the Mn concentration, the lower was the PL intensity rise. The PL intensity increase was 1.5 times for 0.1% of Mn concentration and 2.6:1 molar ratios of MgO to TiO_2 . The effect is ascribed mainly to the increase of concentration of Mn^{4+} ions as well as to the decrease of the influence of non-radiative recombination. The latter presumably occurs through the decrease of energy transfer between the Mn^{4+} ions and/or the decrease of concentration of the

centers of non-radiative recombination. It is proposed that the adding of excess MgO can be used for the improvement of Mn⁴⁺ red PL in magnesium titanate crystal phases.

Acknowledgements This work was partly supported via bilateral program DNIPRO (project M/15-2019 in Ukraine and #42549TM in France) funded by the Ministry of Education and Research of Ukraine, by the Ministries of Foreign Affairs and International Development (MAEDI) and the Ministry of Education, Higher Education and of Research (MENESR) in France, as well as by National Academy of Sciences of Ukraine (project III-10-18). The authors thank Dr. Alexandre Vimont and Dr. Olivier Marie from the Laboratoire Catalyse & Spectrochimie, 6 Boulevard Maréchal Juin, 14050 Caen Cedex 4 FRANCE, for measurements of diffuse reflectance spectra.

References

- Q. Zhou, L. Dolgov, A.M. Srivastava, L. Zhou, Z. Wang, J. Shi, M.D. Dramićanin, M.G. Brik, M. Wu, *J. Mater. Chem. C* **6**, 2652 (2018)
- J. Silver, G.R. Fern, R. Withnall, in *Materials for Solid State Lighting and Displays*, ed. by A. Kitai (Wiley, Chichester, 2017), pp. 91–134.
- D. Chen, Y. Zhou, J. Zhong, *RSC Adv.* **6**, 86285 (2016)
- <https://www.yujiintl.com/>
- T. Ye, S. Li, X. Wu, M. Xu, X. Wei, K. Wang, H. Bao, J. Wang, J. Chen, *J. Mater. Chem. C* **1**, 4327 (2013)
- M.M. Medic, M.G. Brik, G. Drazic, Z.M. Antic, V.M. Lojpur, M.D. Dramićanin, *J. Phys. Chem. C* **119**, 724 (2015)
- S. Kawakita, H. Kominami, K. Hara, *Phys. Stat. Sol. C* **12**, 805 (2015)
- T.-M. Chen, J. T. Luo, United States Patent, US 7,846,350 B2 (2010)
- Z. Qiu, T. Luo, J. Zhang, W. Zhou, L. Yu, S. Lian, *J. Lumin.* **158**, 130 (2015)
- G. Hu, X. Hu, W. Chen, Y. Cheng, Z. Liu, Y. Zhang, X. Liang, W. Xiang, *Mater. Res. Bull.* **95**, 277 (2017)
- J. Long, C. Ma, Y. Wang, X. Yuan, M. Du, R. Ma, Z. Wen, J. Zhang, Y. Cao, *Mater. Res. Bull.* **85**, 234 (2017)
- L. Borkovska, L. Khomenkova, I. Markevich, M. Osipyonok, T. Stara, O. Gudymenko, V. Kladko, M. Baran, S. Lavoryk, X. Portier, T. Kryshab, *J. Mater. Sci.* **29**, 15613 (2018)
- H. Zhang, H. Zhang, J. Zhuang, H. Dong, Y. Zhu, X. Ye, Y. Liu, B. Lei, *Ceram. Int.* **42**, 13011 (2016)
- D. Chen, Y. Zhou, W. Xu, J. Zhong, Z. Ji, W. Xiang, *J. Mater. Chem. C* **4**, 1704 (2016)
- C.-S. Huang, C.-L. Huang, Yu.-c. Liu, S.-k. Lin, T.-S. Chan, H.-W. Tu, *Chem. Mater.* **30**, 1769 (2018)
- Y.X. Pan, G.K. Liu, *J. Lumin.* **131**, 465 (2011)
- M. Peng, X. Yin, P.A. Tanner, M.G. Brik, P. Li, *Chem. Mater.* **27**, 2938 (2015)
- R. Cao, J. Huang, X. Ceng, Z. Luo, W. Ruan, Q. Hu, *Ceram. Int.* **42**, 13296 (2016)
- M.A. Petrova, G.A. Mikirticheva, A.S. Novikova, V.F. Popova, *J. Mater. Res.* **12**, 2584 (1997)
- B.A. Weichler, A. Navrotsky, *J. Sol. State Chem.* **55**, 165 (1984)
- B.E. Warren, *X-ray diffraction* (Dover Publications Inc., New York, 1990)
- L. Wang, Z. Dai, R. Zhou, B. Qu, X.C. Zeng, *Phys. Chem. Chem. Phys.* **20**, 16992 (2018)
- T. Senden, R. J.A. van Dijk-Moes, A. Meijerink, *Light: Science & Applications*, 7, 8 (2018)
- L. Qin, P. Cai, C. Chen, J. Wang, H.J. Seo, *RSC Adv.* **7**, 49473 (2017)
- H.F. Sijbom, J.J. Joos, L.I.D.J. Martin, K. Van den Eeckhout, D. Poelman, P.F. Smet, *ECS J. Solid State. Sci. Technol.* **5**, R3040 (2016)
- M.G. Brik, Y.X. Pan, G.K. Liu, *J. Alloys Compd.* **509**, 1452 (2011)
- <https://www.visual-epr.com>
- G. Kimmel, J. Zabicky, *Solid State Phenom.* **140**, 29 (2008)
- C.-K. Lee, E. Cho, H.-S. Lee, C.S. Hwang, S. Han, *Phys. Rev. B* **78**, 012102 (2008)
- N. Korsunskaya, Y. Polishchuk, M. Baran, V. Nosenko, I. Vorona, S. Lavoryk, S. Ponomaryov, O. Marie, X. Portier, L. Khomenkova, *Front. Mater.* **5**, 23 (2018)
- T. Murata, T. Tanoue, M. Iwasaki, K. Morinaga, T. Hase, *J. Lumin.* **114**, 207 (2005)
- C.W. Struck, W.H. Fonger, *J. Lumin.* **10**, 1 (1975)
- F. Garcia-Santamaria, J.E. Murphy, A.A. Setlur, S.P. Sista, *ECS J. Sol. St. Sci. Technol.* **7**, R3030 (2018)

Publisher's Note Springer Nature remains neutral with regard to jurisdictional claims in published maps and institutional affiliations.